Orclever Proceedings of Research and Development
https://doi.org/10.56038/oprd.v5i1.567
OR CLEVER Science & Research Group

Conference Article

Analysis of Girder Fatigue Strength and Investigation of Wheel Shaft Loads in C-Type Gantry Cranes

Samet Dönerkaya[1*], Kemalettin Kök[2], Cihat Eroğlu[3]

[1] BVS Cranes R&D Center, https://orcid.org/0000-0001-7577-5124, s.donerkaya@bvs.com.tr
[2] BVS Cranes R&D Center, https://orcid.org/0009-0001-8690-1568, kok@bvs.com.tr
[3] BVS Cranes R&D Center, https://orcid.org/0009-0009-3030-6215, c.eroglu@bvs.com.tr
[*] Correspondence: s.donerkaya@bvs.com.tr; Tel.: +90 507 628 00 30

Received 25 October 2024
Received in revised form 15 December 2024
In final form 23 December 2024

4th International Conference on Design, Research and Development (RDCONF 2024)
December 19 - 20, 2024

Reference: Dönerkaya, S., Kök, K., & Eroğlu, C. (2024). Analysis of girder fatigue strength and investigation of wheel shaft loads in C-type gantry cranes. Orclever Proceedings of Research and Development, 5(1), 347-364.

Abstract

Portal cranes are industrial lifting and transportation machines designed to move loads in horizontal and vertical planes in open areas. C-type portal crane is a crane that features a symmetrical axial design and is structurally characterized by the offsetting of the girder construction from the legs by a certain distance. This offset causes the side view, to resemble the letter "C". Depending on the load-carrying capacity, geometry and volume, C-type portal cranes are optimized with a structural design that allows loads to be positioned without contacting the C-type legs. This distinctive feature enables the safe and secure transportation of loads of various sizes and shapes in a wide range of industrial applications.

In this study, the fatigue strength calculations of the girder and wheel shaft, which are key components of a C-type portal crane, were analyzed analytically within the scope of the DIN EN 13001 standard. Stress values occurring in the girder and wheel loads were obtained using the finite element method (FEM) as part of the design process for the C-type portal crane. Considering the stress values on the wheel shaft, the fatigue limits of these components were calculated according to the draft version of the "DIN EN 13001-3-8: Shafts" standard, published in 2021.

https://doi.org/10.56038/oprd.v5i1.567

For the girder construction, fatigue limits were determined from the tables provided in the EN 13001-3-1+A1 standard and compared with the design stresses. The obtained results were analyzed in accordance with the reference past stress parameter (Sn) in order to examine the safety of the beam weld areas and wheel shafts of the C-type gantry crane. It was determined that the girder and wheel shaft meet the safety criteria corresponding to the S6 class past stress parameter. These findings demonstrate that the design complies with the relevant standards and provides sufficient fatigue strength.

Keywords: *C-Type Portal Crane, EN 13001, Fatigue Strength*

1. Introduction

Fatigue in cranes occurs due to the variable and repetitive loads they are subjected to. These loads impact many components, primarily the main structural elements, such as the main girder and wheel shafts. The girder has a construction without structural integrity, assembled using welded plates and fatigue calculations are performed at these weld zones based on the fatigue stress limits defined by crane standards. The corner welds in the joint regions are subjected to multiaxial effects, including shear and bending loads, which contributes to tensile-compressive and shear stresses. In rotating and bending fatigue-exposed parts such as shafts, stress concentrations lead to fatigue damage, especially in the shoulder bottoms and key fields. At sharp cornered transitions, localized stresses can increase several fold, causing potential cracks to propagate rapidly. This condition can develop over time or occur suddenly, leading to damage that may result in significant losses.

In literature numerous studies have been conducted on analyzing the fatigue conditions of cranes, including investigations on runway, main girder construction and wheel shafts. In a study on wheel shaft, critical stress values at the fillet and keyway regions of the shaft were identified using Scanning Electron Microscopy (SEM). It was observed that enlarging the fillet and keyway root radius of the damaged shaft significantly reduced stress levels that caused fatigue damage [1]. A new method was presented for estimating fatigue loads using parameters such as Q-load class, U-working cycle class, and S-historical stress classes based on the Eurocode 3 and EN 13001 standards [2]. The welding of rails on the runway and the increased stress concentrations in the weld areas create potential damage scenarios that could lead to crack formation. Using FEM and analytical techniques, crack detection, 2D crack growth models and analysis, crack propagation in

https://doi.org/10.56038/oprd.v5i1.567

the weld areas at the rail-runway junction, and the damage modes (tensile-shear) causing this propagation have been investigated. Stress intensity factors (Kσ, Kτ) were obtained using numerical methods [3, 4].

In the areas where the girder is welded to the header, section changes occur and the resulting stress concentrations from these section changes create conditions that promote the formation of potential fatigue damage. In a study, fatigue strength parameters in this region, along with fatigue lifetimes related to crack propagation, were investigated using fracture mechanics theory and the finite element method (FEM) [5]. In addition to static calculations, fatigue calculations can also be performed using FEM software. Stress values in the critical areas of a crane and the fatigue lifetimes in these regions were analyzed using FEM [6]. The study emphasizes the importance of fatigue calculations for safe structures and highlights the critical need to determine the fatigue strength of joint weld areas for ensuring structural safety. In another study on potential fatigue damage that may occur in crane system components, loading cycles were calculated, and stress measurements were conducted. In this study, fatigue cycle counts were obtained for a portal crane, demonstrating that the failures occurring in the crane components have a systematic nature and cannot be explained by random causes [7].

This study examines the adequacy of the main components of a C-type portal crane system, namely the carrier beam and wheel shaft, in terms of infinite life. Autodesk Nastran finite element software was used to determine the maximum stress values. Fatigue calculations were performed according to the EN 13001-3-1+A1 standard for the girder and the EN 13001-3-8 standard for the drive wheel shaft. The EN 13001-3-8 standard, published in 2021, is still in draft form and was evaluated in alignment with the parameters used in this study. The final result determines that the carrier beam and drive wheel shaft of the C-type portal crane, with a 10-ton load capacity, possess a safe design when considering the S6 historical stress parameter.

2. Materials and Methods

2.1 C-Type Portal Crane Model Design and Application Methods

The general structure of the portal crane consists of wheels, headers, legs, and a carrier beam. The portal crane is designed for a load capacity of Q_N = 10 tons, with a span distance of L = 10.9 meters. The external load-bearing length (portafo) is designed as L_k = 3.26 meters. The modeled C-type portal crane and the positions of the wheel bearings are shown in Figure 1. The leg on the portafo side is made solely of steel construction, while concrete filling has been applied into the steel construction on the other leg. This concrete

https://doi.org/10.56038/oprd.v5i1.567

fill ensures a more balanced centre of gravity while the system performs lifting operations under nominal load. This design enhances the stability of the crane system, contributing to achieving optimal load capacity.

The leg on the portafo side is made solely of steel construction, while concrete filling has been applied into the steel construction on the other leg. This concrete fill ensures a more balanced centre of gravity while the system performs lifting operations under nominal load. This design enhances the stability of the crane system, contributing to achieving optimal load capacity.

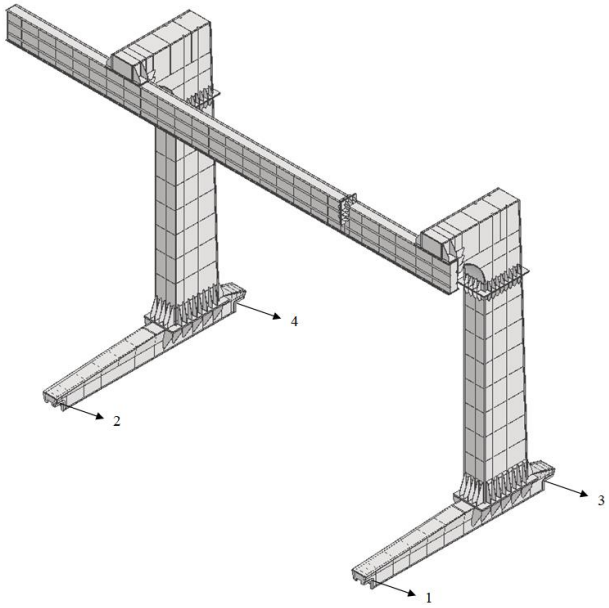

Figure 1: C-Type Portal Crane Model and Positions of Wheel Bearings.

2.2 Analysis of the Crane Structure's Behaviour under Static Load

In the static load analysis, four different loading position scenarios were considered. Position 1 represents the situation where the load is located on the section with concrete fill, Position 2 represents the situation where the load is at the centre of the crane girder, Position 3 represents the situation where the load is on the leg on the portafo side, and Position 4 represents the situation where the load is at the tip of the portafo. The carrying load for the analysis scenarios was determined as Q_N = 10 tons, and the trolley group load was set as Q_A = 0.8 tons. The loading condition was evaluated according to the EN 13001 standard, with the A1 loading condition being considered in the analyses. For fatigue load calculations during loading, a partial safety factor of γ_P = 1 was applied. In addition, other factor coefficients were adapted according to crane operating conditions, and the

https://doi.org/10.56038/oprd.v5i1.567

analyzed load values were determined accordingly [8]. These evaluations provided the opportunity to analyze the behaviour of the C-type portal crane model under static loads in accordance with international standards.

The material used in the production of the C-type portal crane chassis and the carrier beam is S355JR steel alloy. In the analyses conducted with Autodesk Nastran, shell elements were preferred and as a result of mesh convergence, second-degree quadrilateral elements were used as the element type with a total of 214,980 mesh elements and 573,636 nodes. This detailed mesh structure enhanced the accuracy and precision of the analysis results.

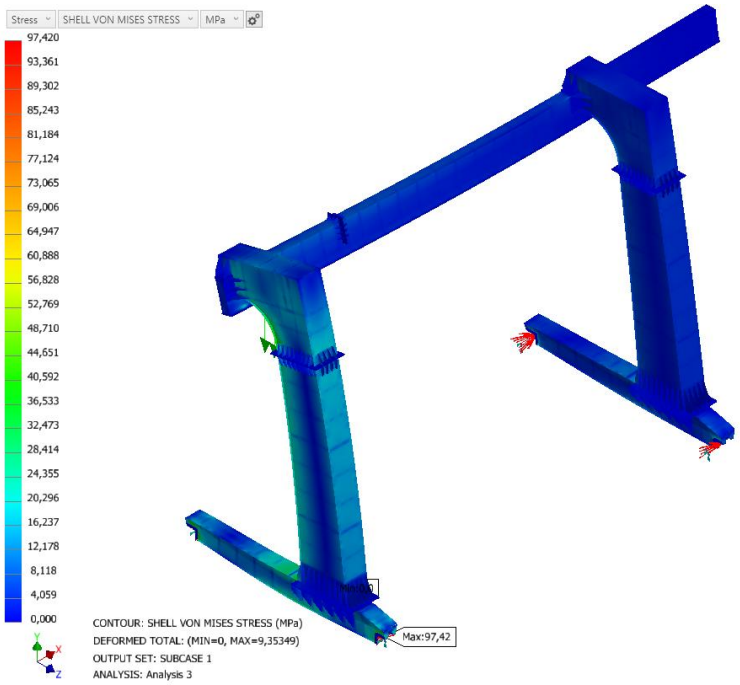

Figure 2. Von Mises Stress Distribution for the Case Where the Nominal Load Is Carried by the Concrete-Filled Leg (Position 1).

https://doi.org/10.56038/oprd.v5i1.567

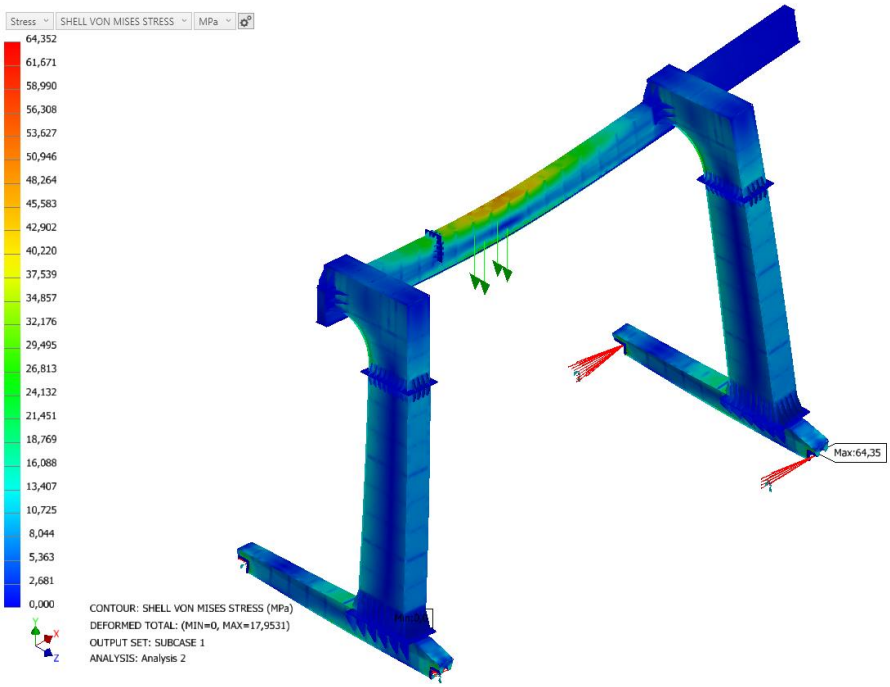

Figure 3. Von Mises Stress Distribution for the Case Where the Nominal Load Is Applied at the Center of the Beam (Position 2).

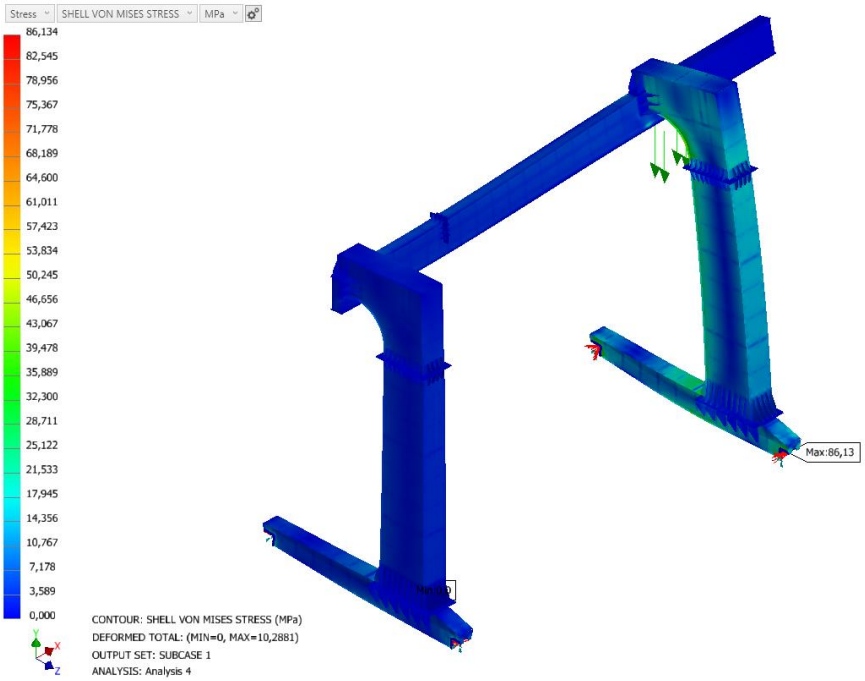

Figure 4. Von Mises Stress Distribution for the Case Where the Nominal Load Is Carried by the Portafo Side of the Leg (Position 3).

https://doi.org/10.56038/oprd.v5i1.567

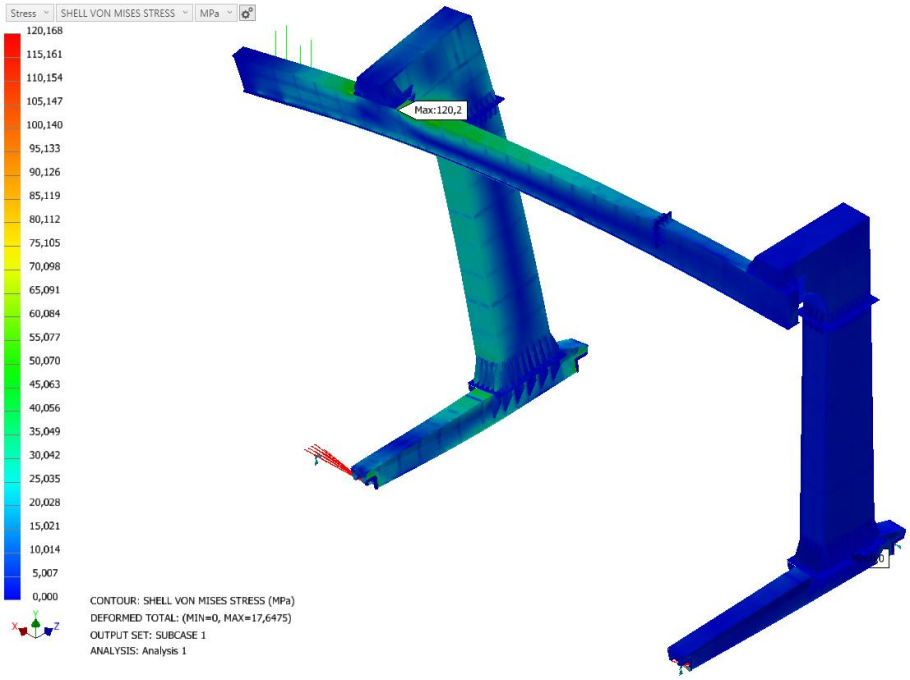

Figure 5. Von Mises Stress Distribution for the Case Where the Nominal Load Is Carried by the End Point of the Portafo (Position 4).

In the analyses conducted for the four different loading positions, the wheel loads and the maximum Von Mises stress values on the beam for each position were calculated in details. The Von Mises stress results obtained for the four loading positions of the C-type portal crane model are illustrated in Figures 2 to 5. According to the results obtained, the highest stress under static loading occurred in Position 4 at the connection region of the beam to the suspension, which calculated as 120 MPa. It was determined that the maximum stress is concentrated at the beam's suspension connection area.

2.3 Analysis and Evaluation of the Fatigue Condition of the Crane Beam

The beam section and welding details of the C-type portal crane are shown in Figure 6. The fatigue limits of a welded connection can be determined, according to the EN 13001-3-1 + A1 standard, by considering the loading types of the parts. In this context, the design of the welded connection and load distributions has been optimized to minimize fatigue limits.

https://doi.org/10.56038/oprd.v5i1.567

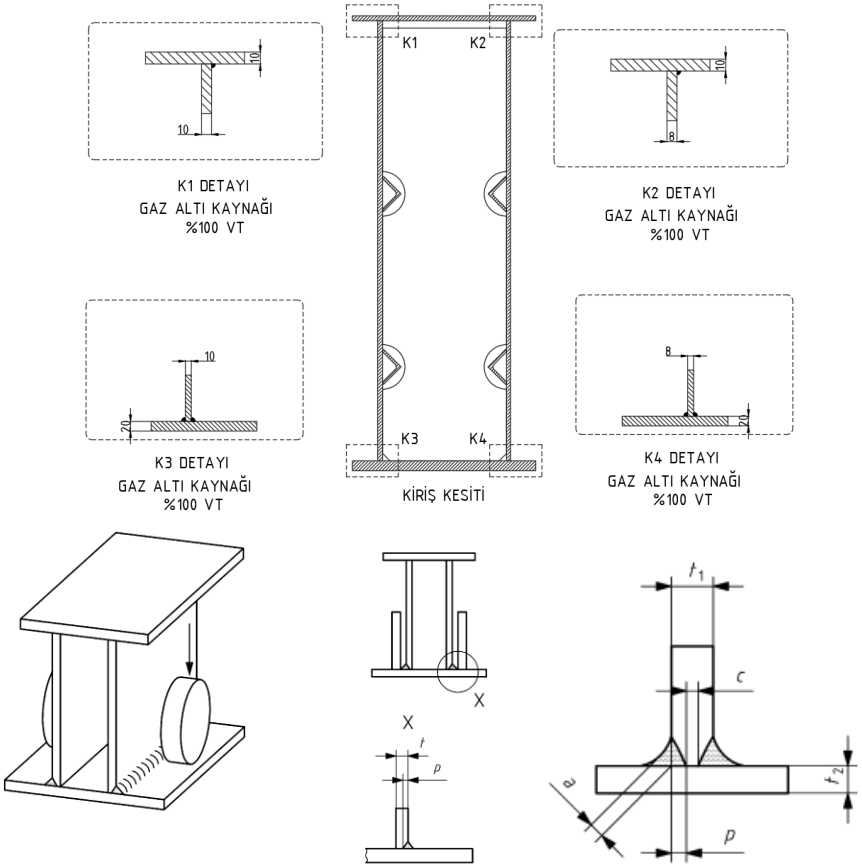

Figure 6. Section and Plate Welding Details of C-Type Portal Crane Beam: EN 13001-3-1+A1-Table D.3-3.16.

The maximum stress values obtained for the beam in different loading positions for the K3 and K4 bottom plate welding regions are presented in Table 1. Here, the minimum stress condition is considered as zero, while the stress condition after loading has been considered as the maximum stress condition.

Table 1. The Maximum and Minimum Stress Values in the Beam under Different Loading Positions

	Position 1	***Position 2***	***Position 3***	***Position 4***
	$\sigma_{Max.} = \sigma_{sd}$	$\sigma_{Max.} = \sigma_{sd}$	$\sigma_{Max.} = \sigma_{sd}$	$\sigma_{Max.} = \sigma_{sd}$
Stress (MPa)	6.8	34.2	7.6	40.3

The maximum stress contours for two critical positions are shown in Figures 7 and 8. According to the analysis results, the highest stress condition occurred in Position 4 (Figure 7). These stresses are particularly concentrated in the lower plate weld regions, playing a critical role in the fatigue strength of the beam.

https://doi.org/10.56038/oprd.v5i1.567

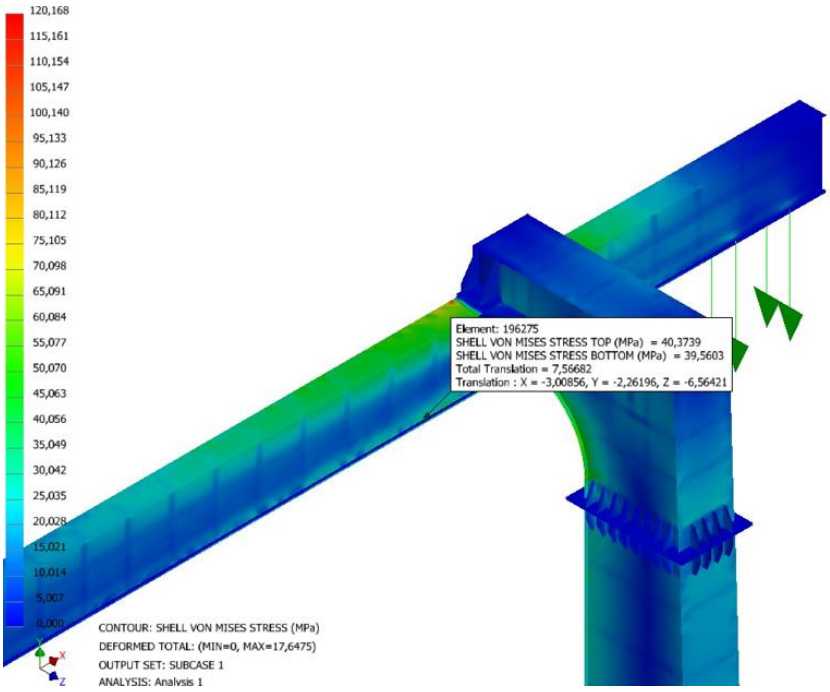

Figure 7. Maximum Stress Contour on the Beam Under Loading Condition Position 4 ($\sigma_{Max.}$= σ_{sd}= 40.3 MPa).

According to the EN 13001-3-1+A1 standard, the characteristic fatigue strength value for the bottom plate weld condition of a single beam is $\Delta\sigma_c$ = 63 MPa, and the limit fatigue strength value $\Delta\sigma_{rd}$ is provided in Table 2. Considering the S6 fatigue class, $\Delta\sigma_{rd}$ was calculated as 63.5 MPa.

https://doi.org/10.56038/oprd.v5i1.567

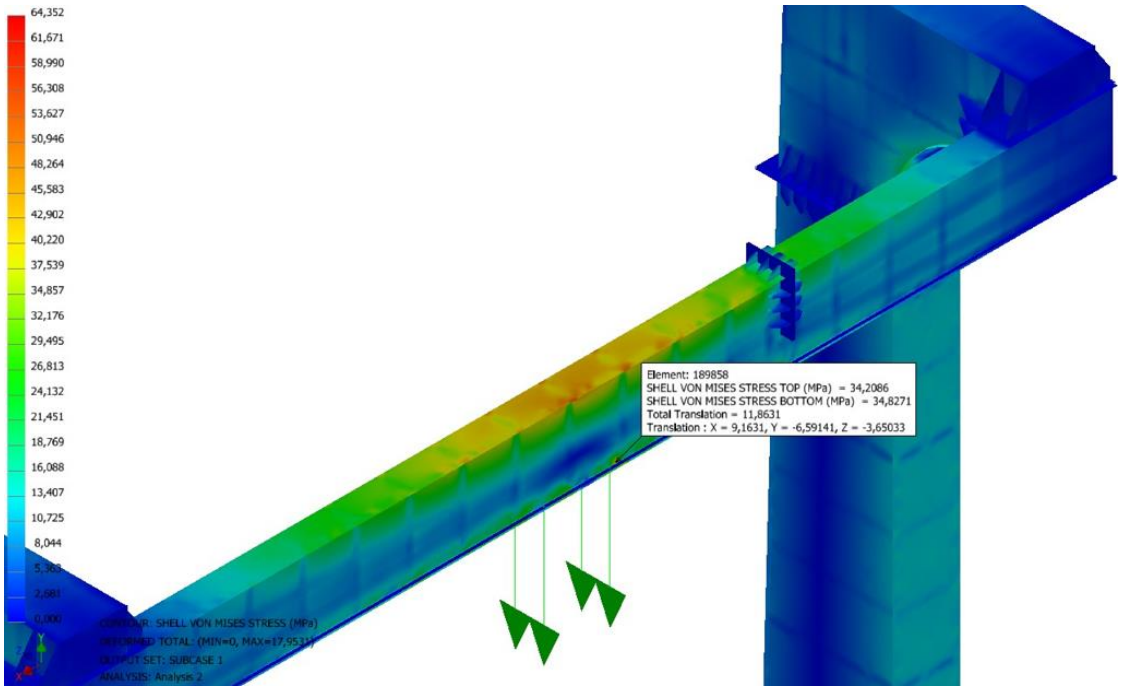

Figure 8. Stress Contour on the Beam under Loading Condition Position 2 ($\sigma_{Max.}$= σ_{sd}= 34.2 MPa).

Table 2. Fatigue Limit Strength Values ($\Delta_{\sigma rd}$) Based on S3 Previous Stress Parameter: Calculated Values in Accordance with EN 13001-3-1 + A1.

NC, m= 3	**S0**	**S1**	**S2**	**S3**	**S4**	**S5**	**S6**	**S7**	**S8**	**S9**
$\Delta\sigma_c$= 63 MPa	252	200	158,8	126,7	100,8	80	***63,5***	50,4	40	31,8

Under fatigue effects, the beam is safe if the value in Table 2 ($\Delta\sigma_{rd}$=63.5 MPa) is greater than the maximum design stress value. Since $\Delta\sigma_{rd}$ = 63.5 MPa > maximum stress (Position 1: 6.7 MPa; Position 2: 34.2 MPa; Position 3: 7.6 MPa; Position 4: 40.3 MPa), the weld connection points of the girder are safe according to the S6 stress parameter and are considered to have an infinite lifespan due to fatigue effects.

2.4 Wheel Shaft Fatigue Calculation and Durability Analysis

The maximum wheel loads obtained for different loading positions are listed in Table 3. These loads were derived from the finite element analysis (FEA) results of the C-type portal crane system, and the forces acting on the wheels, namely Fx, Fy, and Fz, are detailed for each position. Single Point Constraint (SPC) approach was utilized for

https://doi.org/10.56038/oprd.v5i1.567

calculating the forces obtained for each loading position which reflect the effects of the nominal load on the wheel bearings during loading.

Table 3. Calculation of Wheel Loads According to Maximum Load Carrying Capacity and Pose Conditions.

		Maximum Wheel Load (N)			
		Position 1	**Position 2**	**Position 3**	**Position 4**
1th Wheel	F_x	-1931,3	205,7	22729,1	3492,8
	F_y	113945	73605,9	41565,2	22563,7
	F_z	0	0	0	0
2nd Wheel	F_x	0	0	0	0
	F_y	46201,7	75894	107769	126671
	F_z	0	0	0	0
3rd Wheel	F_x	1931,3	-205,7	-2279,1	-3492,8
	F_y	127294	90263,1	59663,8	41437,5
	F_z	-2231,4	168,857	2491	3871,9
4th Wheel	F_x	0	0	0	**0**
	F_y	56026,9	85809	116574	**134899**
	F_z	2231,4	-168,8	-2491	**-3871,9**

Wheel loads will be used as fundamental data to determine the stress distribution on the crane's lifting system and to perform the subsequent fatigue calculations for the wheel shaft. According to the results of the analysis, the maximum wheel load occurred in Position 4 and 4th wheel. These findings not only provide an important guideline for assessing the safety performance of the wheels under critical loading conditions, but also enhancing the reliability of the design. As a result, valuable information regarding the identification of the system's critical areas and ensuring structural safety has been obtained.

In the lifting system of the C-type portal crane, the wheel shaft of the drive group which is subjected to rotational and bending loads, is likely to experience damage due to fatigue in at least 2-3 different critical areas. The loading conditions in the system lead to bending, shear, and torsional stresses on the shaft, as shown in Figure 10, particularly in the critical area of the invoice region in Figure 9, increasing the risk of fatigue.

https://doi.org/10.56038/oprd.v5i1.567

The model and loading condition of the shaft are shown in Figure 9. The stress concentrations in the most critical areas of the shaft were examined in detail for long-term durability. In the reference system, the shaft is driven by a 1.1 kW motor and rotation is provided by a reducer with a nominal torque of 443 Nm. It has been found that driving the shaft with a keyed connection causes the highest stress value to be concentrated at the connection point called the invoice region. This critical area, concerning the durability of the shaft, has been improved by applying heat treatment and annealing processes to the C4140 steel to enhance its material properties. These findings will design improvements to ensure the safe operating life of the shaft.

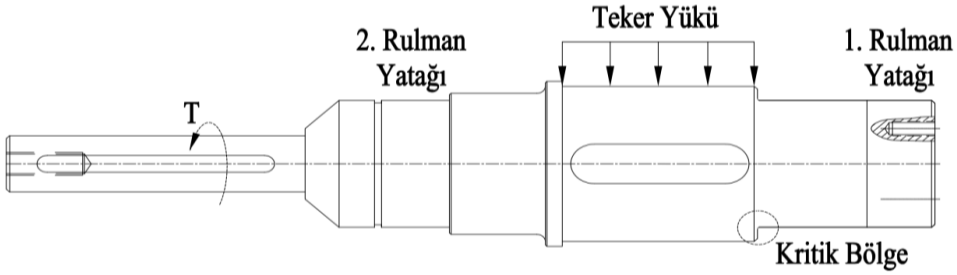

Figure 9. Loading Condition and Model of the Distributed Load Distribution on the Shaft.

Safety condition of wheel shaft under fatigue effects has been checked based on the standard titled "DIN EN 13001-3-8: Shafts," published in December 2021. Based on the maximum wheel load obtained from the wheel loads in Table 1, the static analyses of the shaft were modeled individually. In this model, it was assumed that the shaft is held at the bearing regions and has rotational freedom. The wheel load is defined as a distributed load, as shown in Figure 9. The load is determined as the maximum wheel load (resultant force) from Table 3, which is F_B = 134.908 N. This analysis is a critical step in determining the shaft's load-bearing capacity and safe operating conditions. The necessary safety limits have been established to ensure the shaft's fatigue strength. After the loading condition, the shear (cutting), bending, and torsional stress-position graphs are shown in Figure 10. The obtained values have been calculated using equations [1-4], with the normal stress ⌾sd = 81,8 MPa and the total shear stress $\tau_{sd} = \tau_{max}$ = 13.75.

Table 4 presents the parameters used in the calculation of the fatigue limit value along with the results obtained. The formulas required for calculating each parameter are taken from the EN 13001-3-8 standard, and these formulas are provided in the Appendix section (See Equations 5-19). Based on the results obtained, the fatigue limits of the design have been determined, and the safe operating conditions for the shaft have been defined.

https://doi.org/10.56038/oprd.v5i1.567

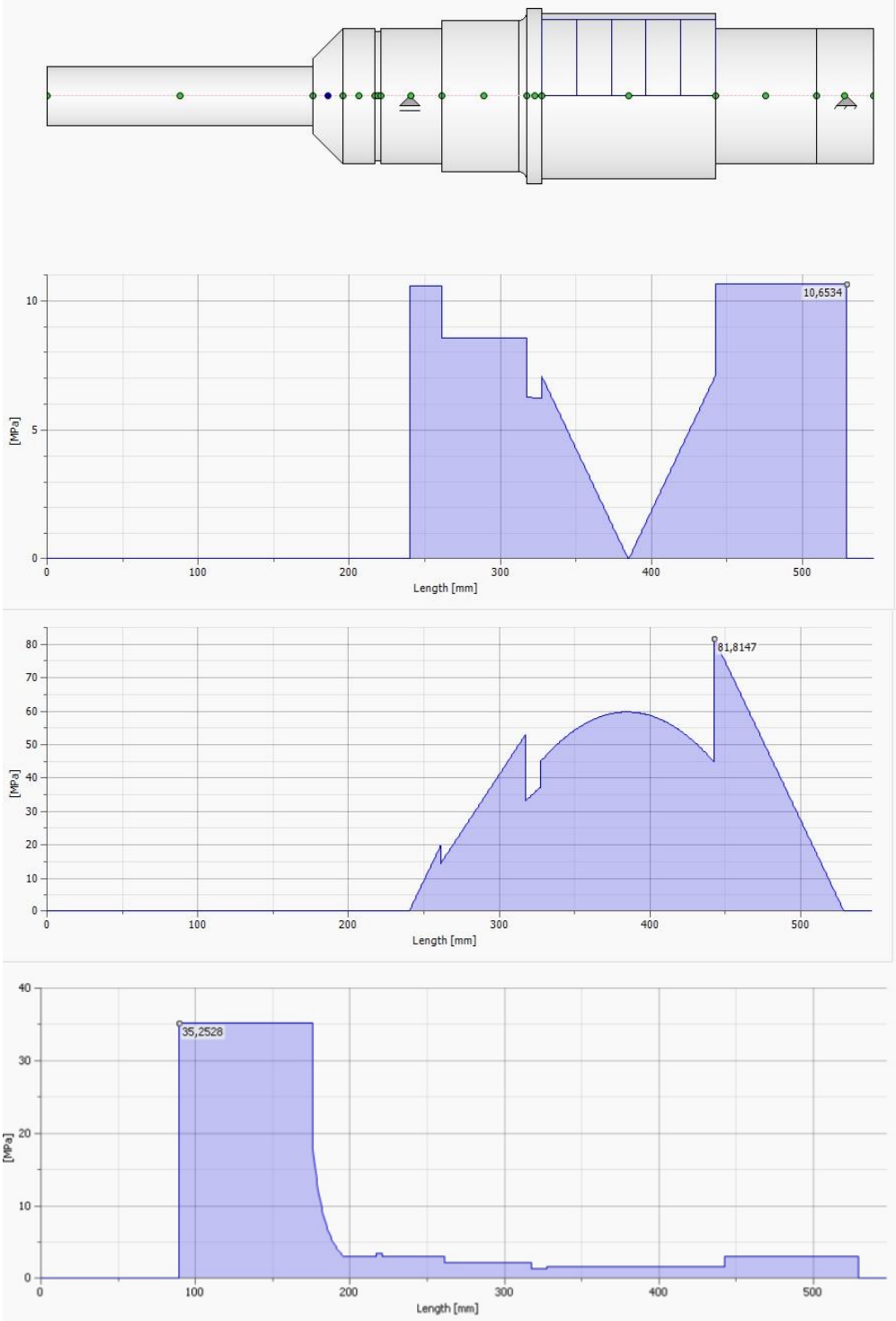

Figure 10. Stress-Position Diagrams under Shear Force (a), Moment (b), and Torsional (c) Loads: Stress Distributions Based on Loading Conditions (Autodesk Inventor Nastran-Design Acc. Module).

https://doi.org/10.56038/oprd.v5i1.567

Table 4. Input Parameters and Calculation Results for Fatigue Strength Calculation.

Index	Value	Unit	Description
$\sigma_{max}=\sigma_{sd}$	81.8	MPa	Maximum Design Stress (Normal)
$\tau_{max}=\tau_{sd}$	13.4	MPa	Maximum Design Stress (Kayma)
σ_m	41.2	MPa	Average Normal Stress
τ_m	6.8	MPa	Average Shear Stress
d	90	mm	Small Diameter of the Invoice
D	110	mm	Large Diameter of the Invoice
r	1	mm	Radius of the Invoice
t	10	mm	Invoice Thickness
f_u	900	MPa	Material Tensile Strength, 42CrMo4
R_a	3.2	µm	Average Roughness Value
S_n	0.5	-	Previous Stress Parameter
γ_{mf}	1.25	-	Original Strength Factor
Kt	3.25	-	Stress Concentration Factor (Bending)
z	0.7	-	Fit Factor
f_1	2.28	-	Notch Factor
f_2	0.76	-	Size Factor
f_3	0.87	-	Surface Roughness Factor
f_4	1	-	Surface Treatment Factor
f_{prob}	0.84	-	* Sustainability factor
σ_{d_ref}	340.2	MPa	Material Fatigue Strength (Normal)
τ_{d_ref}	196.4	MPa	Material Fatigue Strength (Shear)
$\sigma_{d,s}$	98.4	MPa	Variable Fatigue Strength (Normal)
$\tau_{d,s}$	57.2	MPa	Variable Fatigue Strength (Shear)
σ_d	137.6	MPa	Part Fatigue Strength (Normal)
τ_d	63.8	MPa	Part Fatigue Strength (Shear)
m_σ	7.75	-	Fatigue Curve Slope (Normal)
m_τ	6.90	-	Fatigue Curve Slope (Slip)
σ_{Rd_ref}	120.4	MPa	Design Fatigue Limit (Normal)
τ_{Rd_ref}	56.5	MPa	Design Fatigue Limit (Sliding)

* The probability of the component continuing to operate without failure over a specified service life. All indices in the fatigue calculation were derived from the "EN 13001-3-8, Shafts" standard.

https://doi.org/10.56038/oprd.v5i1.567

Based on the calculated design fatigue limits (normal and shear) and the stress values (normal and shear) occurring in the shaft, adequacy of the structure for infinite life ($2x10^6$) can be determined using Equation [1]:

$$\gamma_{ff} = \frac{1}{\sqrt{\left(\frac{\sigma_{sd,f}}{\sigma_{Rd,f}}\right)^2 + \left(\frac{\tau_{sd,f}}{\tau_{Rd,f}}\right)^2}} \quad [1]$$

Where γ_{ff} represents the fatigue safety factor. For a structure to be considered safe, the value of γ_{ff} must be greater than 1 ($\gamma_{ff} > 1$). For the C-type portal crane wheel shaft, the calculated fatigue safety factor is $\gamma_{ff} = 1.38$. This result indicates that, according to the S6 previous stress parameter, the shaft is fatigue-resistant and will have an infinite lifespan.

3. Result

In the study conducted for the carrier beam, it was determined whether the structure was sufficient for infinite life according to the maximum stress value on the bottom plate weld connection details where the monorail crane wheels move. According to the EN 13001-3-1+A1 standard, the fatigue limits for the critical weld areas K3 and K4 have been defined. In the analyses conducted, the stress values in these regions were determined based on different loading positions. The maximum stress values obtained in the different loading position cases should not exceed the defined fatigue limit value; this limit value is $\Delta\sigma_{rd}$ = 63.5 MPa according to the S6 stress parameter. The stress value obtained in the Position 4 loading case is σ_{max} = 40.3 MPa and since it is smaller than ◎◎rd, it is concluded that the carrier beam is sufficient for infinite life.

In this study, the fatigue strengths of the carrier beam and drive wheel shaft, which are important components of the C type gantry crane, were investigated. For the drive shaft, the EN 13001-3-8 standard, which is still in draft form, and for the carrier beam, the EN 13001-3-1+A1 standard were considered. In terms of fatigue, the keyways and the bottom of the shaft are the most critical areas [1]. Reducing the stress concentrations in these areas is of great importance for structural safety. The wheel shaft is subjected to bending and rotational loads. The maximum moment applied to the wheel shaft occurs in the considered invoice area. Therefore, the infinite life calculation in terms of fatigue was carried out in this region. As a result of the fatigue calculations, it was determined that the shaft is safe for infinite life according to the S6 stress history parameter.

According to the results of the analysis, the maximum wheel load occurred in Position 4 and 4th wheel. These findings not only provide an important guideline for assessing the

safety performance of the wheels under critical loading conditions, but also enhancing the reliability of the design. As a result, valuable information regarding the identification of the system's critical areas and ensuring structural safety has been obtained.

When considering both the material properties and the obtained stress values, it can be concluded that the S355JR steel material used in the construction of the C-type portal crane ensures the safety of the structure under static loads. This comprehensive approach guarantees the reliability of the crane system under both static and dynamic loading conditions.

4. Discussion and Conclusion

In this study, the fatigue strength of the wheel shaft and girder in the C-type portal crane system has been investigated, and their suitability for infinite life has been evaluated based on the DIN EN 13001 standard. In industrial applications, static validation alone is not sufficient for the design of cranes used in heavy-duty sectors. These cranes must perform their tasks without any damage occurring over the required service life cycles. The DIN EN 13001 standard defines Sn for service life cycles and establishes stress previous parameters ranging from the heaviest to the lightest workload categories [2]. In this context, fatigue strength calculations are of great importance. Especially for cranes, the fatigue limits of key components such as the beam and wheel shaft, which are exposed to load, can be determined using various analytical approaches. Nowadays, fatigue calculations can be carried out using analytical methods, as well as through finite element analysis approaches that include different fatigue calculation methods. Crane manufacturers are planning to use more computer-aided software in the near future to increase their competitive edge. Specifically, it is anticipated that fatigue calculations will be carried out using finite element software.

References

[1] Domazet, Ž., Lukša, F., & Bugarin, M. (2014). Failure of Two Overhead Crane Shafts. Engineering Failure Analysis, 44, 125-135.

[2] Euler, M., & Taylor, C. (2021). Fatigue Action on Crane Runway Beams. Journal of Constructional Steel Research, 181, 106476.

[3] Rettenmeier, P., Roos, E., Weihe, S., & Schuler, X. (2016). Assessment Of Mixed Mode Crack Propagation Of Crane Runway Girders Subjected To Cyclic Loading. Engineering Fracture Mechanics, 153, 11-24.

https://doi.org/10.56038/oprd.v5i1.567

[4] Ávila, G., Palma, E., & De Paula, R. (2017). Crane Girder Fatigue Life Determination Using SN and LEFM Methods. Engineering Failure Analysis, 79, 812-819.

[5] Zhao, X., Jin, N., Liu, X., & Shi, Z. (2022). Fatigue Failure Analysis Of Steel Crane Beams With Variable-Section Supports. Engineering Failure Analysis, 136, 106217.

[6] Buczkowski, R., & Żyliński, B. Finite Element Fatigue Analysis Of Unsupported Crane. Polish Marit. Res. 28 (1), 127–135 (2021).

[7] Kopnov, V. A. (1999). Fatigue Life Prediction of The Metalwork Of A Travelling Gantry Crane. Engineering Failure Analysis, 6(3), 131-141.

[8] EUROPEAN STANDARD, EN 13001-2:2014, Crane Safety - General Design - Part 2: Load Actions.

[9] EUROPEAN STANDARD, EN 13001-3-1+A1:2013, Cranes - General Design - Part 3-1: Limit States and Proof Competence Of Steel Structures.

[10] EUROPEAN STANDARD, EN 13001-3-8 Cranes - General Design - Limit States And Proof Competence Of Machinery - Part 3-8: Shafts.

https://doi.org/10.56038/oprd.v5i1.567

Appendix

$$\sigma_{B=}\frac{32M}{\pi D^3} \quad [1]$$

$$\tau_{P=}\frac{4F}{\pi D^2} \quad [2]$$

$$\tau_{T=}\frac{16T}{\pi D^3} \quad [3]$$

$$\sigma_B = \sigma_{mak,} \qquad \tau_{mak=}\tau_p+\tau_T \quad [4]$$

$$\sigma_{m=}\frac{\sigma_{mak}+\sigma_{min}}{2} \quad [5]$$

$$\tau_{m=}\frac{\tau_{mak}+\tau_{min}}{2} \quad [6]$$

$$\sigma_{d_{ref}=}\,0{,}45\times f_u\times f_{prob} \quad [7]$$

$$\sigma_{d,s} = \sigma_{d,ref} * \left(\frac{f_2 * f_3 * f_4}{f_1}\right) \quad [8]$$

$$\tau_{d,s} = \tau_{d,ref} * \left(\frac{f_2 * f_3 * f_4}{f_1}\right) \quad [9]$$

$$\tau_{d_{ref}=}\frac{\sigma_{d,ref}}{\sqrt{3}} \quad [10]$$

$$K_t = 1 + \frac{1}{\sqrt{0{,}62 * \frac{r}{t} + 11{,}6 * \frac{r}{d} * \left(1 + 2 * \frac{r}{d}\right)^2 + 0{,}2 * \left(\frac{r}{d}\right)^3 * d/D}} \quad [11]$$

$$f_1 = z\ x\ K_t \quad [12]$$

$$f_2 = 9{,}308 * d^{-0{,}0065} - 0{,}0116 * \sqrt{d} - 8{,}169 \quad [13]$$

$$f_3 = 1 - 0{,}22 * log\frac{R_a}{0{,}4} * (log\frac{f_u}{200}) \quad [14]$$

$$f_4 = 1{,}2 * \left(\frac{25 - d}{45}\right) + 1 \quad [15]$$

$$\sigma_d = 2 * \left(\frac{f_u - \sigma_{d,s}}{2 * f_u - \sigma_{d,s}}\right) * \sigma_m + \sigma_{d,s} \quad [16]$$

$$\tau_d = \tau_{d,s} + \tau_m \quad [17]$$

$$\sigma_{Rd,f=}\frac{\sigma_d}{\gamma_{Mf}\times^{m_\sigma}\sqrt{s_s}} \quad [18]$$

$$\tau_{Rd,f=}\frac{\tau_d}{\gamma_{Mf}\times^{m_\tau}\sqrt{s_s}} \quad [19]$$